Organic Electronics 85 (2020) 105820

Contents lists available at ScienceDirect

Organic Electronics

journal homepage: http://www.elsevier.com/locate/orgel

AIEE based "turn-on" fluorescent sensor for Al^{3+} ions and induced tetraphenylethene self-assemblies

Zejun Xu [a,1], Yanan Liu [a,1], Ruitong Wang [a], Junheng Zhang [a], Juan Cheng [a], Sufang Chen [b], Menghe Miao [c], Daohong Zhang [a,*]

[a] Key Laboratory of Catalysis and Energy Materials Chemistry of Ministry of Education & Hubei Key Laboratory of Catalysis and Materials Science, Hubei R&D Center of Hyperbranched Polymers Synthesis and Applications, South-Central University for Nationalities, Wuhan, 430074, China
[b] Key Laboratory for Green Chemical Process of Ministry of Education, Hubei Key Laboratory of Novel Reactor and Green Chemical Technology, School of Chemical Engineering and Pharmacy, Wuhan Institute of Technology, Wuhan, Hubei, 430205, China
[c] CSIRO Manufacturing, 75 Pigdons Road, Waurn Ponds, Victoria, 3216, Australia

ARTICLE INFO

Keywords:
Self-assembly
AIEE
Carbohydrazide derivative
Fluorescence sensor

ABSTRACT

Cu^{2+} is an eminent trace metal ion in the human body as a structural cofactor that can enhance immune function. Aluminum is one of the most abundant elements found in the earth's crust and most biological tissues appear in Al^{3+} form. Hg^{2+} is probable to cause cancer with high toxicity. However, excess accumulation of Al^{3+}, Cu^{2+} or Hg^{2+} in the body leads to many diseases. Therefore, detecting the level of Al^{3+}, Cu^{2+} and Hg^{2+} are very important for human health. However, preparing a suitable single probe for the simultaneous detection of Al^{3+}, Cu^{2+} and Hg^{2+} remains a challenge. TPE-based carbohydrazide derivative (TPE-Ch) was synthesized by the one-pot reaction. The TPE-Ch displayed notable AIE and AIEE phenomena and can act as a fluorescence sensor that turns on toward Al^{3+} in ethanol/water mixtures (f_w = 70%) and turns off toward Cu^{2+} or Hg^{2+}. TPE-Ch can produce various assemblies by coordination with Al^{3+}, Cu^{2+} and Hg^{2+}, including nanospheres, tree-like assembly morphology and belt-like superstructures. Optical microscopy (OM), scanning electron microscopy (SEM), X-ray diffraction (XRD), and fluorescence spectrography were employed to characterize the self-assemblies.

1. Introduction

A multifunctional probe that changes selective recognition of multiple ions offers great application prospects [1,2]. Cu^{2+} is an eminent trace metal ion in the human body as a structural cofactor that can enhance immune function [3,4]. Aluminum exists in most organisms in the form of Al^{3+}. However, excess accumulation of Cu^{2+}or Al^{3+} in the body leads to many diseases [5], and Hg^{2+} is probable to cause cancer with high toxicity [6,7]. Therefore, detecting the level of Al^{3+}, Cu^{2+} and Hg^{2+} are very important for human health. Recently, several fluorescent probes for the selective recognition of Al^{3+}, Cu^{2+} or Hg^{2+} have been reported [1,8–11]. The pyrene-appended pyrazoline compound (PY–I) displayed an excellent sensitive response to Al^{3+} [10]. The tetraphenylethylene derivative (probe 2) showed sensitive response to Cu^{2+}, with detection limit of 0.5 μM [9]. Yongfeng Zhou group reported the self-assembly of alternating copolymer vesicles for the highly selective and sensitive of aqueous Hg^{2+}, and the detection limit is about 53 nM [8]. However, it is still a challenge to prepare a suitable single probe for the simultaneous detection of Al^{3+}, Cu^{2+} and Hg^{2+} [12,13].

Recently, aggregation induced emission (AIE) of tetraphenylethylene (TPE) molecules have been used in various fields, such as biological probes [14–17], chemical sensing, optoelectronic systems [18,19], and self-assembly systems [20,21]. TPE based micro/nano-structures, such as fibers, nanowires, microflowers, and their applications were investigated [22–28]. Therefore, it would be of great interest to synthesize a TPE derivative for the simultaneous detection of Al^{3+}, Cu^{2+} and Hg^{2+} and to investigate Al^{3+}, Cu^{2+}/Hg^{2+}-induced TPE self-assembly.

Herein, we have successfully designed and synthesized TPE-based carbohydrazide derivative (TPE-Ch) that displays AIE phenomena and AIEE properties with fluorescence-sensing capability that "turns-on" for Al^{3+} ions and "turns-off" for Cu^{2+}/Hg^{2+}. TPE-Ch could produce various assemblies by coordination with Al^{3+}, Cu^{2+} and Hg^{2+}, including nanospheres, tree-like assembly morphology and belt-like superstructures. We hypothesized that the intermolecular π-π stacking, the integration of

* Corresponding author.
E-mail address: zhangdh27@163.com (D. Zhang).
[1] These authors contributed equally to this work.

https://doi.org/10.1016/j.orgel.2020.105820
Received 15 January 2020; Received in revised form 25 May 2020; Accepted 25 May 2020
Available online 4 June 2020

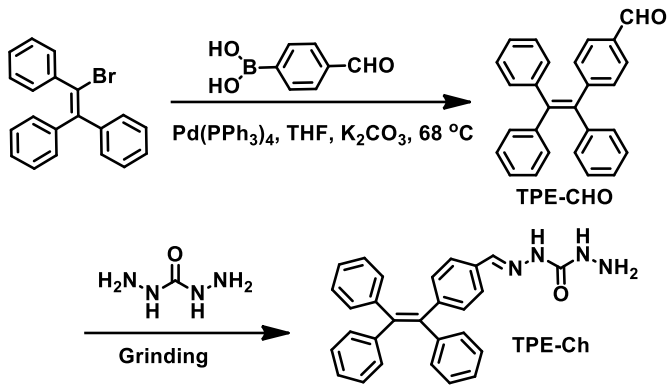

Scheme 1. Synthesis route of TPE-Ch.

metal coordination along with other H-bonding are the key drivers in the self-assembly processes.

2. Experimental section

Preparation for fluorescence measurements: TPE-Ch (10 mM) stock solution was prepared in EtOH. The solution of TPE-Ch was then diluted to 10 μM for fluorescence spectral researches with EtOH/water mixed solvents having different water fractions (f_w: changing from 0% to 90%). Stock solutions of K^+, Na^+, Ca^{2+}, Al^{3+}, Zn^{2+}, Cu^{2+}, Cd^{2+}, Fe^{3+}, and Hg^{2+} (10 mM) were dissolved in distilled water. Fluorescence response of TPE-Ch (10 μM) with different concentrations of Al^{3+}, Cu^{2+} and Hg^{2+} (0–200 μM) in water-EtOH mixtures (f_w = 70%) were determined. The samples in a quartz cell of 10 mm path length, exciting at 355 nm wavelength and using a slit width of 5 nm having an integration time of 0.1 s to record emission scans from 370 to 700 nm.

Preparation for self-assembly samples: TPE-Ch (500 μM) was dissolved in ethanol solvent mixed with Hg^{2+} or Cu^{2+}. The self-assembly was performed on a clean surface of the glass substrate. The morphology of the self-assemblies was recorded using optical microscopy (OM) at 500× magnification and scanning electron microscopy (SEM).

3. Results and discussion

TPE-Ch was synthesized according to Scheme 1 [29]. TPE-CHO was prepared by modifying a method reported in the literature [30] with 90% yield as shown in Scheme 1. TPE-CHO was then grounded with carbohydrazide to form the carbohydrazide derivative TPE-Ch in 85% yield as an off-white powder. TPE-Ch was characterized by ^{1}H NMR and LC-TOF mass spectrometry in the supplementary information.

To determine the AIE feature of TPE-Ch, the emission behavior of the compound in the ethanol/water system was investigated [31]. Fig. 1 shows the photoluminescent (PL) emission spectra of TPE-Ch in ethanol/water mixtures with different water fractions (f_w). Obviously, with the increase of f_w ($f_w \leqq 60\%$), the weak emission intensity of TPE-Ch increases slightly and the fluorescence peak red-shifted from 450 to 467 nm. However, when $f_w > 60\%$, the emission intensity enhanced dramatically and exhibited a red-shift to 485 nm (f_w = 90%), showing about tenfold enhancement at f_w = 90% compared with that in pure ethanol solution (Fig. 1b). This suggests a remarkable AIE property (Scheme 2) [32,33]. Even in solid-state, this TPE-Ch displayed strong bluish-green emission with a maximum at 488 nm.

The selectivity of TPE-Ch to various metal ions (K^+, Na^+, Ca^{2+}, Al^{3+}, Cu^{2+}, Zn^{2+}, Cd^{2+}, Hg^{2+} and Fe^{3+}) was examined in ethanol/water (f_w = 70%) solution. The fluorescence spectra were obtained by excitation at 355 nm. The major turn-on fluorescence of TPE-Ch was showed in the addition of Al^{3+} while turn-off by presented of Hg^{2+}or Cu^{2+}. As shown in Fig. 2, the probes themselves showed fluorescence emission at 484 nm. The emission enhancement of TPE-Ch increased gradually with increasing Al^{3+} concentration (0–100 μM) and reached 3-fold when

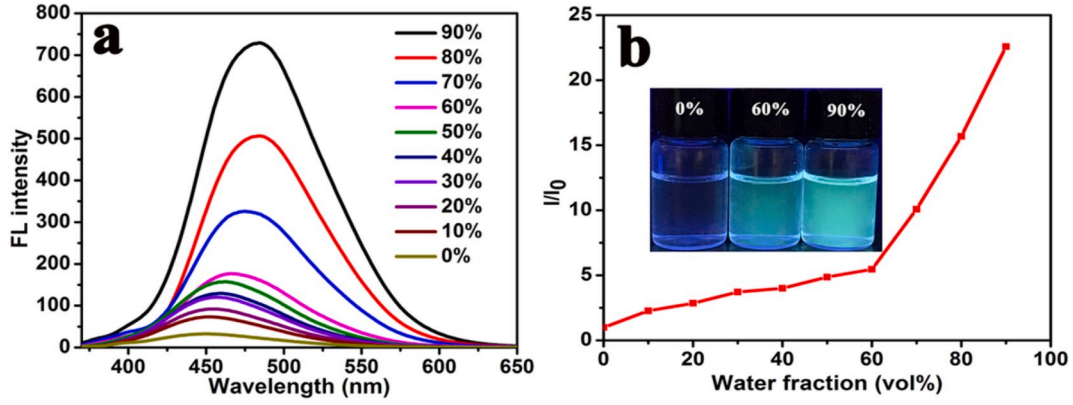

Fig. 1. (a) Fluorescence spectra of TPE-Ch (10 μM, λ_{Ex}: 355 nm) in ethanol-water mixtures (EtOH/H_2O) with different water fractions (f_w). (b) Plots of I/I_0 *vs* f_w of TPE-Ch, where I = emission intensity of f_w, and I_0 = emission intensity in ethanol solution. Inset: images of TPE-Ch at f_w=0%, 60% and 90% under UV lamp.

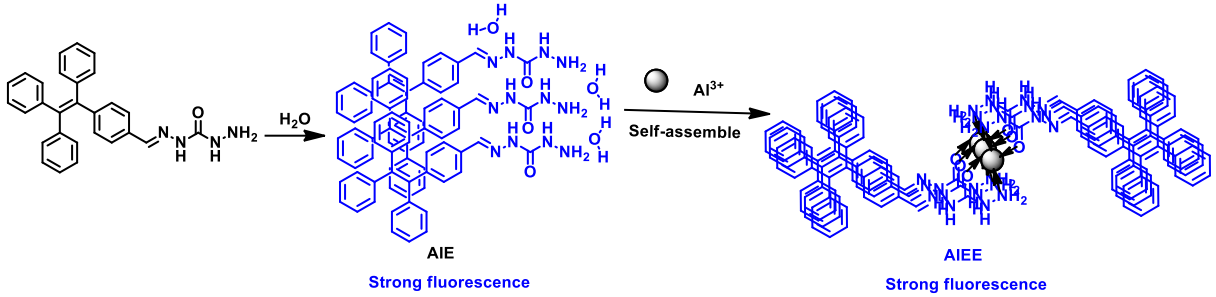

Scheme 2. TPE-Ch displayed AIE phenomena and AIEE properties based "turn-on" for Al^{3+}.

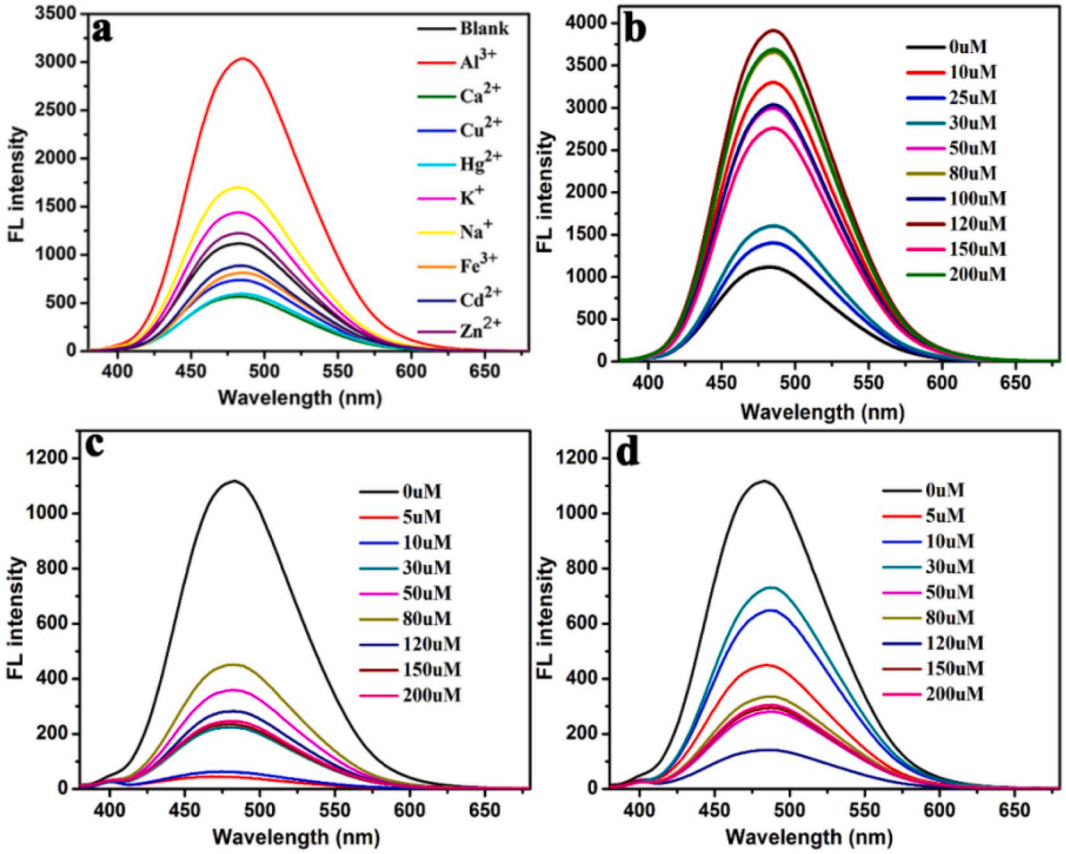

Fig. 2. (a) Fluorescence spectra of TPE-Ch (10 μM) with various metal ions (K^+, Na^+, Ca^{2+}, Al^{3+}, Cu^{2+}, Zn^{2+}, Cd^{2+}, Hg^{2+} and Fe^{3+}) in ethanol/water mixtures (f_w = 70%). Fluorescence spectra of TPE-Ch (10 μM) with increasing concentrations (0–200 μM) of (b) Al^{3+}, (c) Cu^{2+} and (d) Hg^{2+} in ethanol/water mixtures (f_w = 70%).

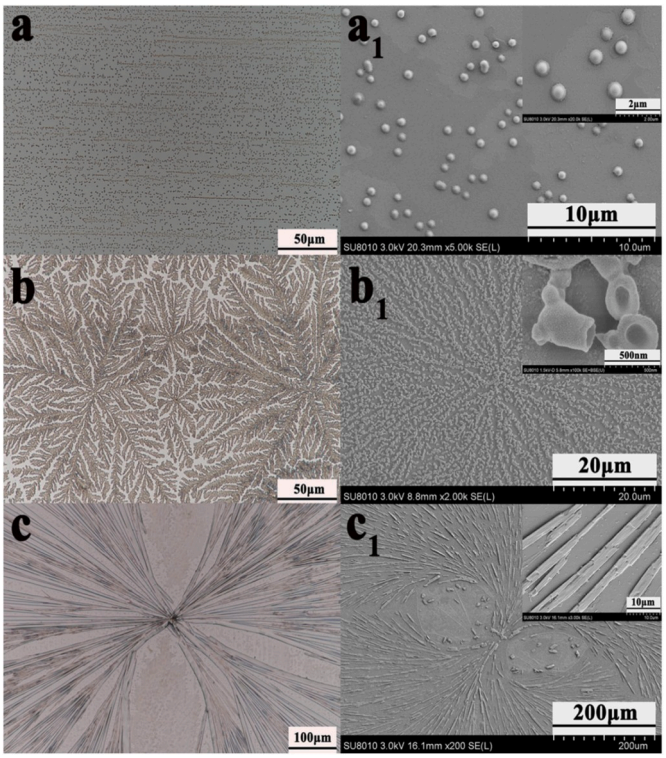

Fig. 3. a-c) Optical micrographs (OM) and a_1-c_1) corresponding scanning electron microscope (SEM) images of (a-a_1) TPE-Ch, (b-b_1) TPE-Ch-Hg^{2+} and (c-c_1) TPE-Ch -Cu^{2+} self-assemblies.

added 5 equiv. of Al^{3+} at 484 nm due to the AIEE effect (Scheme 2) [29]. Nevertheless, a significant decrease in fluorescence intensities of TPE-Ch due to gradual addition of Cu^{2+} or Hg^{2+}, which supports further self-assembly of TPE-Ch induced by Cu^{2+} or Hg^{2+}. The detection limit for Al^{3+}, Cu^{2+} and Hg^{2+} were estimated to be 2.5, 1.6 and 3.5 μM, respectively. Conversely, slight effect on fluorescence was observed after the addition of other cations (K^+, Na^+, Zn^{2+}, Fe^{3+} and Cd^{2+}). In ethanol/water mixtures (f_w = 0%), the $\boldsymbol{\Phi}_f$ of TPE-Ch was 14.66%. In ethanol/water mixtures (f_w = 70%), the $\boldsymbol{\Phi}_f$ of TPE-Ch, TPE-Ch-Al^{3+}, TPE-Ch-Hg^{2+}, TPE-Ch-Cu^{2+} were 16.29%, 15.87%, 32.81% and 28.24% respectively. In ethanol/water mixtures (f_w = 0%), the lifetime of TPE-Ch was 2.45 ns? In ethanol/water mixtures (f_w = 70%), the lifetime of TPE-Ch, TPE-Ch-Al^{3+}, TPE-Ch-Hg^{2+}, TPE-Ch-Cu^{2+} were 6.46 ns, 6.93 ns, 6.81 ns and 7.39 ns respectively. And the sensing time limit for Al^{3+}, Cu^{2+} and Hg^{2+} were 3, 10 and 12 s, respectively.

The self-assembly behaviors of TPE-Ch before and after adding metal ions (including Cu^{2+}, Hg^{2+}, Al^{3+}, Ca^{2+}, K^+, Ba^{2+}, Mg^{2+}, and Zn^{2+}) were studied by an OM and SEM. Metal ions with different coordination modes might have helped the assembly growth. As the EtOH solvent slowly volatilized at a temperature under 25 °C and relative humidity 50%, the self-assemblies of TPE-Ch before and after adding metal ions (including Al^{3+}, Ca^{2+}, K^+, Ba^{2+}, Mg^{2+}, and Zn^{2+}) under the OM appeared as small spheres with uniform size and close arrangement (Fig. 3a). The SEM images further showed that with the volatilization of the solvent it assembled into nanospheres with diameters in the range of 500–800 nm (Fig. 3a_1). However, after adding Hg^{2+}, we observed that the small particles displayed regular patterns of a snowflake- or tree-like assemblies (Fig. 3b). Subsequently, the SEM analysis revealed that the branches of the tree were assembled from hollow nanoparticles (inset in Fig. 3b_1), probably self-assembly caused by induction of Hg^{2+}. As shown in Fig. 3c, the addition of Cu^{2+} causes the self-assembly morphology of

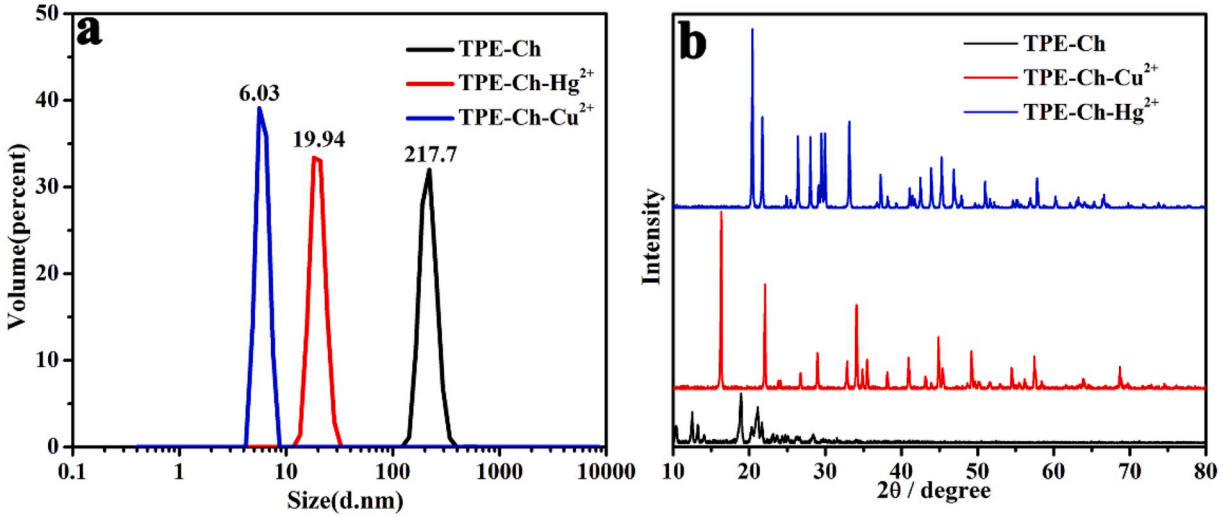

Fig. 4. (a) Dynamic light scattering (DLS)-based particle size analysis of self-assemblies. (b) X-ray diffraction (XRD) spectra of TPE-Ch, TPE-Ch-Cu^{2+} and TPE-Ch-Hg^{2+}.

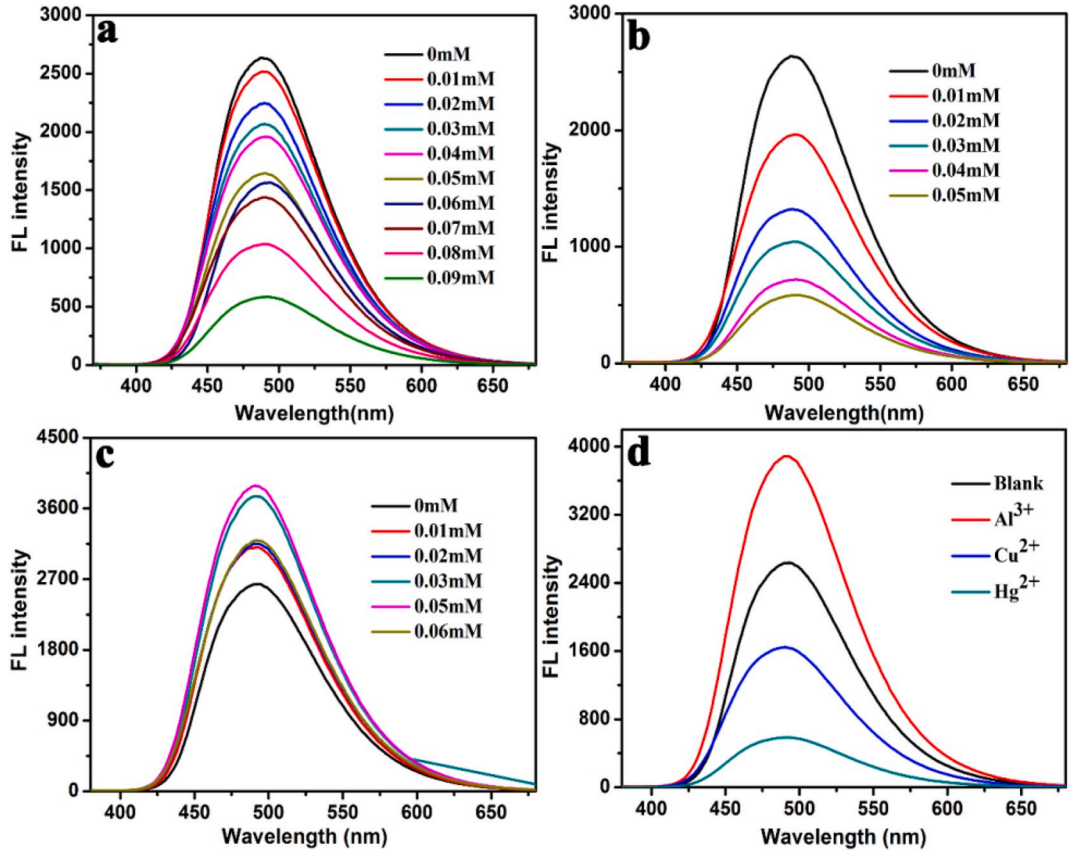

Fig. 5. Fluorescence spectra of TPE-Ch (100 μM) with increasing amounts of (a) Cu^{2+}, (b) Hg^{2+} and (c) Al^{3+} in solid-state. (d) Fluorescence spectra of TPE-Ch (100 μM) with various metal ions (Al^{3+}, Cu^{2+}, and Hg^{2+}) in solid-state.

TPE-Ch to change from sphere to one-dimensional belt-like superstructures formed by bundles of fibers longer than 800 μm. The SEM image confirmed that the fibre bundles were comprised of spliced long fibre sheets (Fig. 3c_1), which are generally several micrometers wide and tens of micrometers long. Thus the metal ions had a great influence on the assembly morphology of the TPE-Ch system.

As discussed above, metal ions (Hg^{2+} and Cu^{2+}) played a vital role in inducing self-assembly. DLS and XRD were used to elucidate the assembly mechanism (Fig. 4). DLS is a very suitable method to investigate the time sequence of self-assembly, which monitors the dispersed or aggregated state of molecules. As shown in Fig. 4a, the self-assembly particle size after adding Cu^{2+} and Hg^{2+} decreased to 19.9 nm and 6.0 nm from 217.7 nm in the initial TPE-Ch solution in ethanol solvent. These results are consistent with the observation obtained from the OM and SEM analyses. The XRD pattern of TPE-Ch revealed a crystalline material giving peaks at 13.7°, 18.5°, and 20.9°, indicating that a strong

π-π stacking interaction exists in the TPE cores of TPE-Ch assembly [31, 34]. The XRD patterns displayed sharp peaks for self-assemblies of TPE-Ch-Cu^{2+} and TPE-Ch-Hg^{2+}, which confirmed well-ordered crystalline structures. What surprised us was that the diffraction peaks and peak intensities in the XRD spectra of self-assemblies of TPE-Ch, TPE-Ch-Cu^{2+} and TPE-Ch-Hg^{2+} were completely different. We hypothesize that the intermolecular π-π stacking, the integration of metal coordination and other H-bonding interactions are the main driving forces in these self-assembly processes.

To further investigate the self-assembly properties, the fluorescence spectra of TPE-Ch with increasing concentrations of Cu^{2+}, Hg^{2+} and Al^{3+} in solid states were studied (Fig. 5). Upon addition of Cu^{2+} or Hg^{2+} to TPE-Ch in solid states by solvent evaporation, the fluorescence emission at 488 nm of TPE-Ch gradually decreased (Fig. 5a and b), resulting in an obvious fluorescence quenching. While addition of Al^{3+} to TPE-Ch in solid states, the fluorescence emission gradually enhanced (Fig. 5c), suggesting a remarkable AIEE property. The major turn-on fluorescence of TPE-Ch in solid states was showed in the addition of Al^{3+} while turn-off by presented of Hg^{2+}or Cu^{2+} (Fig. 5d), this result further supports the conclusion that the self-assembly of TPE-Ch was induced by Cu^{2+} or Hg^{2+} or Al^{3+}, consistent with the results obtained from the fluorescence spectra of TPE-Ch with increasing concentrations of Cu^{2+}, Hg^{2+} and Al^{3+} in ethanol/water ($f_w = 70\%$) solution.

4. Conclusions

A TPE-based carbohydrazide derivative (TPE-Ch) was synthesized by a one-pot reaction with high yield. It displayed notable AIE and AIEE phenomena. TPE-Ch exhibits sensitivity toward Al^{3+} with 3-fold fluorescence enhancement in ethanol/water mixtures at $f_w = 70\%$. TPE-Ch could produce various assemblies by coordination with Al^{3+}, Cu^{2+} and Hg^{2+}, including nanospheres, tree-like assembly morphology and belt-like superstructures. OM, SEM, XRD and fluorescence spectrography were employed to characterize the self-assemblies. The integration of metal coordination, along with other H-bonding and π-π stacking interactions, played a crucial role in these assemblies.

Declaration of competing interest

There are no conflicts of interest to declare.

Acknowledgment

We gratefully acknowledge the financial support of the National Natural Science Foundation of China (51703250 and 51873233), the Innovation Group of Hubei Natural Science Foundation (2018CFA023), the Fundamental Research Funds for the Central Universities, South-Central University for Nationalities (CZQ20009, CZP20006 and CZP18001).

Appendix A. Supplementary data

Supplementary data to this article can be found online at https://doi.org/10.1016/j.orgel.2020.105820.

References

[1] M. Ghosh, S. Mandal, S. Ta, D. Das, Detection and discrimination of Al^{3+} and Hg^{2+} using a single probe: nano-level determination, human breast cancer cell (MCF7) imaging, binary logic gate development and sea fish sample analysis, Sens. Actuators, B 249 (2017) 339–347.
[2] X. Chen, T. Pradhan, F. Wang, J.S. Kim, J. Yoon, Fluorescent chemosensors based on spiroring-opening of xanthenes and related derivatives, Chem. Rev. 112 (2012) 1910–1956.
[3] Q. Niu, T. Sun, T. Li, Z. Guo, H. Pang, Highly sensitive and selective colorimetric/fluorescent probe with aggregation induced emission characteristics for multiple targets of copper, zinc and cyanide ions sensing and its practical application in water and food samples, Sens. Actuators, B 266 (2018) 730–743.
[4] M.G. Choi, Y.J. Lee, I.J. Chang, H. Ryu, S. Yoon, S.-K. Chang, Flatbed-scanner-based colorimetric Cu^{2+} signaling system derived from a coumarin-benzopyrylium conjugated dye, Sens. Actuators, B 268 (2018) 22–28.
[5] J. Cho, T. Pradhan, Y.M. Lee, J.S. Kim, S. Kim, A calix[2]triazole[2]arene-based fluorescent chemosensor for probing the copper trafficking pathway in Wilson's disease, Dalton Trans. 43 (2014) 16178–16182.
[6] W. Fang, G. Zhang, J. Chen, L. Kong, L. Yang, H. Bi, J. Yang, An AIE active probe for specific sensing of Hg^{2+} based on linear conjugated bis-Schiff base, Sens. Actuators, B 229 (2016) 338–346.
[7] S. Yoon, E.W. Miller, Q. He, P.H. Do, C.J. Chang, A bright and specific fluorescent sensor for mercury in water, cells, and tissue, Angew. Chem. Int. Ed. 46 (2007) 6658–6661.
[8] T. Rasheed, C. Li, F. Nabeel, W. Huang, Y. Zhou, Self-assembly of alternating copolymer vesicles for the highly selective, sensitive and visual detection and quantification of aqueous Hg^{2+}, Chem. Eng. J. 358 (2019) 101–109.
[9] A. Sen Gupta, K. Paul, V. Luxami, A fluorescent probe with "AIE+ESIPT" characteristics for Cu^{2+} and F^- ions estimation, Sens. Actuators, B 246 (2017) 653–661.
[10] M. Rangasamy, K. Palaninathan, A pyrazoline-based fluorescent chemosensor for Al3+ ion detection and live cell imaging, New J. Chem. 42 (2018) 10891–10897.
[11] G. Kumar, K. Paul, V. Luxami, Aggregation induced emission-excited state intramolecular proton transfer based "off-on" fluorescent sensor for Al^{3+} ions in liquid and solid state, Sens. Actuators, B 263 (2018) 585–593.
[12] A. Rai, A.K. Singh, K. Tripathi, A.K. Sonkar, B.S. Chauhan, S. Srikrishna, T. D. James, L. Mishra, A quick and selective rhodamine based "smart probe" for "signal-on" optical detection of Cu^{2+} and Al^{3+} in water, cell imaging, computational studies and solid state analysis, Sens. Actuators, B 266 (2018) 95–105.
[13] H. Kim, B.A. Rao, J.W. Jeong, S. Mallick, S.-M. Kang, J.S. Choi, C.-S. Lee, Y.-A. Son, A highly selective dual-channel Cu^{2+} and Al^{3+} chemodosimeter in aqueous systems: sensing in living cells and microfluidic flows, Sens. Actuators, B 210 (2015) 173–182.
[14] X. Zhang, K. Wang, M. Liu, X. Zhang, L. Tao, Y. Chen, Y. Wei, Polymeric AIE-based nanoprobes for biomedical applications: recent advances and perspectives, Nanoscale 7 (2015) 11486–11508.
[15] X. Zhang, X. Zhang, B. Yang, M. Liu, W. Liu, Y. Chen, Y. Wei, Polymerizable aggregation-induced emission dye-based fluorescent nanoparticles for cell imaging applications, Polym. Chem. 5 (2014) 356–360.
[16] R. Jiang, M. Liu, T. Chen, H. Huang, Q. Huang, J. Tian, Y. Wen, Q.-y. Cao, X. Zhang, Y. Wei, Facile construction and biological imaging of cross-linked fluorescent organic nanoparticles with aggregation-induced emission feature through a catalyst-free azide-alkyne click reaction, Dyes Pigments 148 (2018) 52–60.
[17] J. Chen, M. Liu, Q. Huang, L. Huang, H. Huang, F. Deng, Y. Wen, J. Tian, X. Zhang, Y. Wei, Facile preparation of fluorescent nanodiamond-based polymer composites through a metal-free photo-initiated RAFT process and their cellular imaging, Chem. Eng. J. 337 (2018) 82–90.
[18] T. Tao, Y. Gan, Y. Zhao, J. Yu, Q. Huang, Z. Yang, M. Chen, W. Huang, Triphenylethylene-based biimidazoles showing preferable detection of explosives and their rhenium complexes undergoing chiral and cis-trans transformations, J. Mater. Chem. C 7 (2019) 3765–3771.
[19] T. Tao, Y. Gan, J. Yu, W. Huang, Tuning aggregation-induced emission properties with the number of cyano and ester groups in the same dibenzo[b,d]thiophene skeleton for effective detection of explosives, Sens. Actuators, B 257 (2018) 303–311.
[20] J. Mei, N.L.C. Leung, R.T.K. Kwok, J.W.Y. Lam, B.Z. Tang, Aggregation-Induced Emission: together we shine, united we soar!, Chem. Rev. 115 (2015) 11718–11940.
[21] J. Mei, Y. Hong, J.W.Y. Lam, A. Qin, Y. Tang, B.Z. Tang, Aggregation-induced emission: the whole is more brilliant than the parts, Adv. Mater. 26 (2014) 5429–5479.
[22] W.Z. Yuan, F. Mahtab, Y. Gong, Z.-Q. Yu, P. Lu, Y. Tang, J.W.Y. Lam, C. Zhu, B. Z. Tang, Synthesis and self-assembly of tetraphenylethene and biphenyl based AIE-active triazoles, J. Mater. Chem. 22 (2012) 10472–10479.
[23] H.-T. Feng, S. Song, Y.-C. Chen, C.-H. Shen, Y.-S. Zheng, Self-assembled tetraphenylethylene macrocycle nanofibrous materials for the visual detection of copper(ii) in water, J. Mater. Chem. C 2 (2014) 2353–2359.
[24] R. Hu, J.W.Y. Lam, H. Deng, Z. Song, C. Zheng, B.Z. Tang, Fluorescent self-assembled nanowires of AIE fluorogens, J. Mater. Chem. C 2 (2014) 6326–6332.
[25] H.-Q. Peng, X. Zheng, T. Han, R.T.K. Kwok, J.W.Y. Lam, X. Huang, B.Z. Tang, Dramatic differences in aggregation-induced emission and supramolecular polymerizability of tetraphenylethene-based stereoisomers, J. Am. Chem. Soc. 139 (2017) 10150–10156.
[26] D.D. La Anuradha, M. Al Kobaisi, A. Gupta, S.V. Bhosale, Chiral assembly of AIE-active achiral molecules: an odd effect in self-assembly, Chem. Eur J. 23 (2017) 3950–3956.
[27] Y. Li, Y. Dong, X. Miao, Y. Ren, B. Zhang, P. Wang, Y. Yu, B. Li, L. Isaacs, L. Cao, Shape-controllable and fluorescent supramolecular organic frameworks through aqueous host-guest complexation, Angew. Chem. Int. Ed. 57 (2018) 729–733.
[28] Z. Xu, Y. Liu, C. Qian, L. Wu, Z. Wu, J. Zhang, J. Cheng, M. Miao, D. Zhang, Tuning the morphology of melamine-induced tetraphenylethene self-assemblies for melamine detecting, Org. Electron. 76 (2020) 105476.
[29] W.-N. Wu, P.-D. Mao, Y. Wang, X.-J. Mao, Z.-Q. Xu, Z.-H. Xu, X.-L. Zhao, Y.-C. Fan, X.-F. Hou, AEE active Schiff base-bearing pyrene unit and further Cu^{2+}-induced self-assembly process, Sens. Actuators, B 258 (2018) 393–401.

[30] X. Zhao, C. Ji, L. Ma, Z. Wu, W. Cheng, M. Yin, An Aggregation-Induced Emission-based "turn-on" fluorescent probe for facile detection of gaseous formaldehyde, ACS Sens. 3 (2018) 2112–2117.
[31] B. Xu, W. Li, J. He, S. Wu, Q. Zhu, Z. Yang, Y.-C. Wu, Y. Zhang, C. Jin, P.-Y. Lu, Z. Chi, S. Liu, J. Xu, M.R. Bryce, Achieving very bright mechanoluminescence from purely organic luminophores with aggregation-induced emission by crystal design, Chem. Sci. 7 (2016) 5307–5312.
[32] E. Wang, E. Zhao, Y. Hong, J.W.Y. Lam, B.Z. Tang, A highly selective AIE fluorogen for lipid droplet imaging in live cells and green algae, J. Mater. Chem. B 2 (2014) 2013–2019.
[33] X. Feng, Y. Li, X. He, H. Liu, Z. Zhao, R.T.K. Kwok, M.R.J. Elsegood, J.W.Y. Lam, B. Z. Tang, A substitution-dependent light-up fluorescence probe for selectively detecting Fe^{3+} ions and its cell imaging application, Adv. Funct. Mater. 28 (2018) 1802833.
[34] Y. Liu, Z. Xu, J. Zhang, J. Cheng, M. Miao, D. Zhang, Tuning morphology and functionality of two-component self-assembly induced by H-bond and π-π stacking, Dyes Pigments 170 (2019) 107586.